Journal of
Bionanoscience
Vol. 12, 1–11, 2018

Molecular Docking Studies and ADMET Properties of New 1.2.3 Triazole Derivatives for Anti-Breast Cancer Activity

Mebarka Ouassaf[1], Salah Belaidi[1,*], Khaled Lotfy[2], Ismail Daoud[3], and Houmam Belaidi[1,4]

[1] *Group of Computational and Pharmaceutical Chemistry, LMCE Laboratory, Department of Chemistry, Faculty of Sciences, University of Biskra, 07000, Biskra, Algeria*
[2] *University College of Taiyma, Tabuk University, Tabuk, Saudi Arabia*
[3] *Laboratory of Naturals Products and Bio Actives, Department of Chemistry, Faculty of Sciences, Aboubakr Belkaid University, Tlemcen, Algeria*
[4] *Institut des Sciences Chimiques de Rennes, UMR 6226 CNRS-Université de Rennes 1, Campus de Beaulieu, 35042, Rennes Cedex, France*

Aromatase inhibitors have emerged as promising candidates for the treatment of breast cancer, which represents the second most prevalent cancer in females and is considered as the second leading cause of death among women. Inhibitory effect of 1.2.3 triazole were evaluated on the human aromatase enzyme and compared with the Letrozole (LTZ), the most potent inhibitor of aromatase, which is used as anti-estrogen for breast cancer treatment. For this study MOLEGRO software was used to calculate inhibition energy (IE) of triazoles on aromatase enzyme p450 (3EQM.PDB). As a result we suggest p450–1.2.3 triazole complex has higher stability and stronger affinity because p450 shows more favorable interaction energy. Moreover, Molinspiration and ADMETSAR web servers used to calculate ADMET and physicochemical properties of the target compounds.

Keywords: Molecular Docking, ADMET, Breast Cancer, Aromatase Inhibitors.

RESEARCH ARTICLE

1. INTRODUCTION

Cancer[1] is the leading cause of death worldwide, accounting for an estimated 7.6 million deaths in 2008.[2] Breast cancer is the most common type of cancer in women for both developed and developing countries. The effectiveness of anti-hormonal treatment of early breast cancer can be attributed to the fact that approximately two-thirds of breast tumors are hormone-dependent and require growth factors like estrogen to grow.[3] There is some different type of systemic therapy for breast cancer, one kind is hormonal therapy. Hormonal therapy can be given to women whose breast cancers test positive for estrogen to lower estrogen levels. Letrozole is a third generation of non-steroidal aromatase inhibitor—one class of hormonal therapy drugs—that was first introduces by Novartis to the market as Femara® for the treatment of local or metastatic breast cancer.[4–6]

This study is precisely on aromatase inhibitors as these inhibitors play a central role in the treatment of breast cancer.[7] Estrogen is important and promotes the growth and survival of normal and cancer epithelial cells. The chemical compound estrogen binds to the estrogen receptor (ER) and the activation of the cell progression takes place. The active estrogen receptor tends to bind with promoter gene present in the nucleus, which regulates the gene activity and translates the protein.[8–10] The activated receptor in turn binds to gene promoters in the nucleus and activates many other genes.[11] The activated gene products are thereby responsible for cell division, inhibition of cell death, new blood vessels formation and protease activity. Rapid expression of estrogen receptor is found at earlier stages of breast cancer. Nearly 70% cancer mainly depends on the over-expression of estrogen receptor.[12, 13]

Triazoles are common pharmacophore found in a diverse range of biologically active molecules due to their potential structural features (i.e., capability of hydrogen bonding, stable to metabolic degradation and less undesired effects).[14] Among the AIs, letrozole and anastrozole, both containing 1,2,4-triazole ring, were approved by the Food and Drug Administration (FDA) and they are used

*Author to whom correspondence should be addressed.

as the first-line therapy in the treatment of breast cancer in postmenopausal women since they have been shown to be superior to tamoxifen. Based on the AIs, the triazole ring plays a pivotal role in chelation with heme iron.[15] Along the line, Touaibia group has studied on an aromatase inhibitory activity of various substituted-1,2,3-triazole letrozole-based analogs.[16] The results revealed that 1,2,3-triazole analog of letrozole showed equipotent activity to the parent compound. In addition, the 1,4-disubstituted-1,2,3-triazole was shown to be the most potent compound (IC50 = 1.36 μM) among the tested 1,4-disubstituted-1,2,3-triazole series. However, the interaction mode of the 1,4-disubstituted-1,2,3-triazole series with the target enzyme[17] remains to be explored.

In spite of good therapeutic potentials afforded by existing AIs, there are still ample opportunities for improving the bioactivities of these inhibitors. Therefore, this calls for the search for novel highly potent chemotypes possessing robust aromatase inhibition and drug-like properties. The analysis by Lipinski et al.[14] on oral drugs in their formulation of the well-known "rule of five" has immense impact for drug discovery efforts.

In the present work, the potential of the aromatase inhibitors, letrozole and 1.2.3 triazole Derivatives in the treatment of breast cancer has been analyzed using computational approach.[18–21] This paper reports docking studies for a series of 1,2,3-triazole compounds to investigate the nature of interactions contributing to the biological activities the ability of these compounds to serve as aromatase inhibitors for breast cancer treatment. However, the current study was further extended to prediction of *in silico* parameters like some molecular properties, bioactivity scores for predicting oral bioavailability.

Molecular docking is a computational procedure that attempts to predict the no covalent binding of a macromolecule (Receptor) obtained from data banks or MD simulations, etc. with a small molecule (Ligand) as a lead for further drug development. The lead candidates can be found using a docking algorithm that tries to identify the optimal binding mode of a small molecule to the active site of a macromolecular target.[21]

The docking of aromatase inhibitors and 1.2.3 triazole with human placental aromatase cytochrome P450 reveals the role of amino acid, not only at the active site but also at the molecular or atomic level interaction of these compounds.

The AMDET properties of drugs,[22,23] together with its pharmacological properties[24] are conventionally viewed as a part of drug development. The best ligands after docking analysis were subjected to predict.

2. MATERIAL AND METHODS

2.1. Enzyme Structure

The X-ray crystal structures of human placental aromatase cytochrome P450 in complex with androstenedione

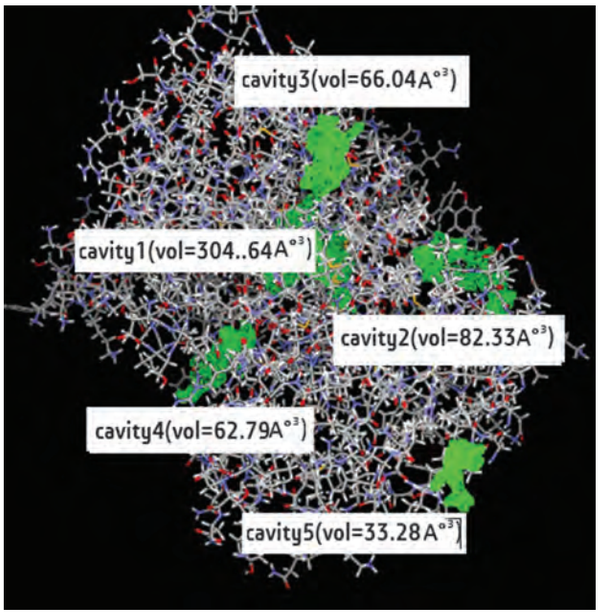

Fig. 1. The five cavities MVD-detected cavities.

(4-ANDROSTENE-3-17-DIONE $C_{19}H_{26}O_2$ AEMFNILZOJDQLW-QAGGRKNESA-N) (PDBID:3EQM)[25] were downloaded from RCSB Database (http://www.rcsb.org/pdb).

Computational analysis was carried out on chain A of 3EQM. 3EQM is a three-dimensional structure with EC Number: EC#: 1.14.14.14, chains (A), resolution 2.90 Å, and *R*-value 2.44 (Fig. 1).

Fig. 2. Secondary structure of the target.

RESEARCH ARTICLE

2.2. Ligand Structures

All ligand structures of 1,2,3-triazole derivatives[26] were optimized by using MM+ molecular modeling and the semi-empirical AM1 method, both of which are implemented in HyperChem 7.0 software (version 7.0, Hypercube, USA, http://www.hyper.com). For these calculations, the Polak–Ribiere conjugate gradient algorithm was employed, with the RMS gradient set to 0.0001 kcal/(Å · mol).

2.3. Cavity Prediction

All cavities or the potential ligand binding site of 3EQM was predicted using MVD. As it is shown in Figure 1. A cavity which has an important volume 151.04 $Å^3$ and a surface area of 462.08 $Å^2$ was predicted and used in our study.

The binding site was set inside a restriction sphere of 15 radiuses with the center *X*: 12.67, *Y*: −3.46, *Z*: 14.09. The MolDock grid score was set with a grid resolution of 0.30.

2.4. Molecular Docking Simulation

In the present investigation, we make use of a docking algorithm called MolDock. So, MolDock is based on a new hybrid search algorithm, called guided differential evolution. The guided differential evolution algorithm combines the differential evolution optimization technique with a cavity prediction algorithm. The use of predicted cavities during the search process, allows for a fast and accurate identification of potential binding modes (poses). We used MVD because it showed higher docking accuracy than other stages of the docking products MVD: 87%, Glide: 82%, Surflex: 75%, FlexX: 58%) in the market.[17, 18]

Molecular docking technique was employed to dock some novel derivatives of 1,2,3-triazole designed L1–L29 (Fig. 3) against p450 receptor 3EQM using MVD to locate the interaction between various compounds and active site of aromatase. MVD requires the receptor and ligand coordinates in either Mol2 or PDB format. Non polar hydrogen atoms were removed from the receptor file and their

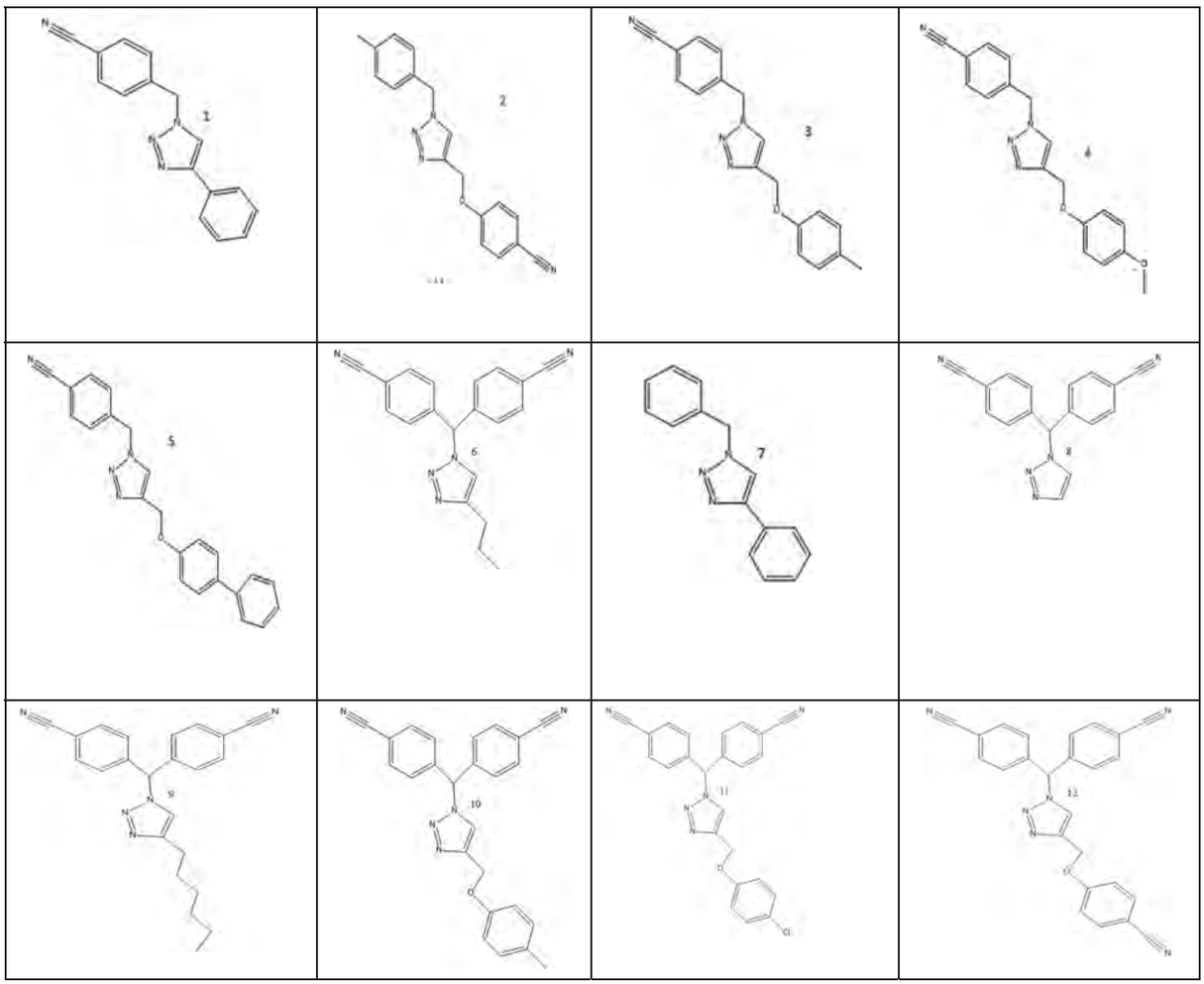

Fig. 3. Continued.

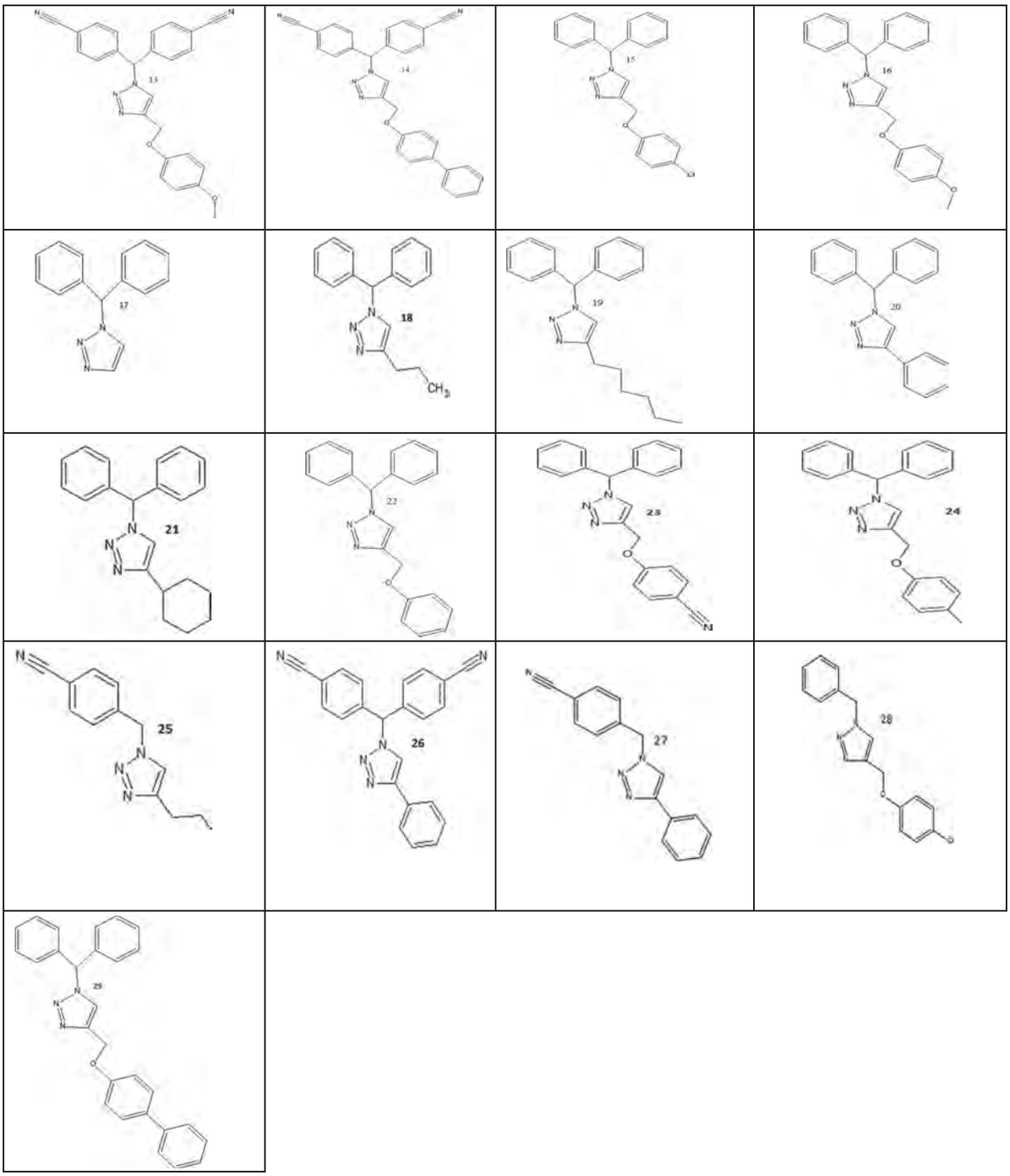

Fig. 3. Chemical structures of the 1.2.3 triazole derivatives.

partial charges were added to the corresponding carbon atoms.

In the docking simulations with MVD, the pose with the minimum MolDock score value was selected as the best solution and for creating two dimensional representations of interactions between ligand and enzyme, LigPlot+ software was used.

Molecular docking was performed using MolDock docking engine of Molegro software. The binding site was defined as a spherical region which encompasses all protein atoms within 15.0 Å of bound crystallographic ligand atom (dimensions *X* (85.67 Å), *Y* (51.14 Å), *Z* (43.73 Å) axes, respectively). Default settings were used for all the calculations.

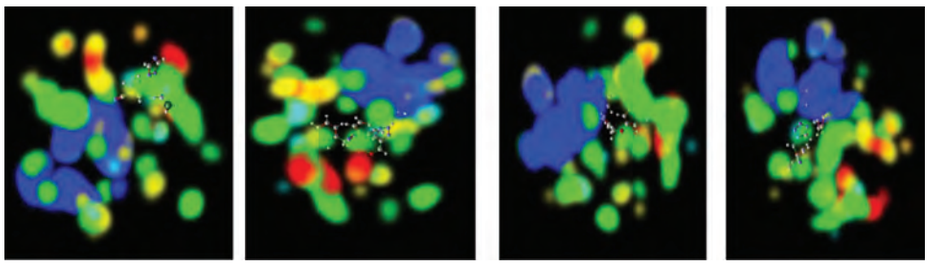

Fig. 4. Energy map of most active compounds and letrozole lat the binding cavity of 3EQM.

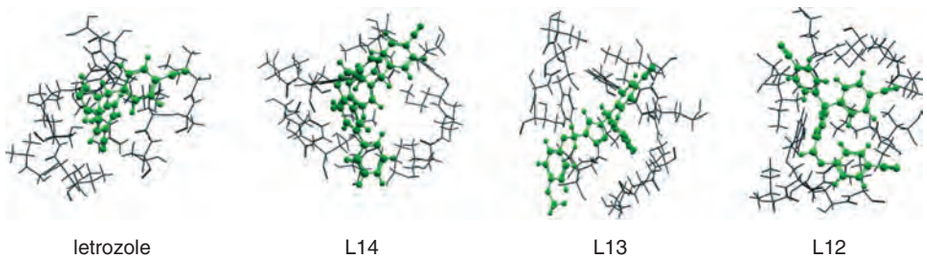

Fig. 5. Pose organize between human placental aromatase cytochrome P450 and most active compounds and letrozole.

Docking was performed using a grid resolution of 0.3 Å and for each of the 10 independent runs; a maximum number of 1500 interactions were executed on a single population of 50 individuals.

2.5. Molecular Property Prediction

Molecular descriptors and drug likeliness properties of compounds were analyzed using the tool Molinspiration server (http://www.molinspiration.com), based on Lipinski Rules of five.[29] According to Lipinski's rule of five, poor absorption or permeation is more likely when there are more than 5 H-bond donors, 10 H-bond acceptors, the molecular weight is greater than 500 Da and the calculated Log*P* (*C*Log*P*) is greater than 5 (or *M*log*P* > 4.15).[27] Moreover, good bioavailability is more likely for compounds with ≤10 rotatable bonds (nrotb) and total polar surface area (TPSA) of ≤140 Å (rule of Veber).[30]

2.6. Prediction of ADMET Properties

The pharmacokinetic properties such as Absorption, Distribution, Metabolism, Excretion and the Toxicity of the compounds can be predicted using the ADMETSAR (http://www.admetexp.org) database. However, BBB (Blood-Brain Barrier) penetration, HIA (Human Intestinal Absorption), Caco-2 cell permeability and Ames test were calculated using the ADMETSAR. In the ADMETSAR, web based query tools incorporating a molecular build-in interface enable the database to be queried by SMILES and structural similarity search. It provides the latest and most comprehensive manually curated data for diverse chemicals associated with known ADMET profiles (ADMETSAR@LMMD).[31]

Table I. Docking results of 3EQM enzyme with of the compounds studied and letrozole.

Ligand	Mol dock score (Kcal/mol)	Interaction (Kcal/mol)	H-bond (Kcal/mol)	Steric energy (Kcal/mol)
1	−114.854	−120.09	−2.44	3.32
2	−137.39	−141.36	−9.73	1.25
3	−142.30	−156.73	−5.02	11.26
4	−143.99	−151.37	−5.69	5.56
5	−138.84	−138.25	−6.11	−3.94
6	−134.71	−137.38	−3.56	0.69
7	−103.71	−110.53	−2.82	6.39
8	−118.15	−124.06	−5.57	3.96
9	−152.84	−155.29	−6.87	2.91
10	−152.71	−150.93	−1.74	6.57
11	−132.77	−146.23	−1.10	10.50
12	−165.80	−169.00	−5.08	1.66
13	−165.01	−178.04	−7.92	6.44
14	−179.89	−189.90	−5.22	6.94
15	−130.14	−140.23	−4.70	8.91
16	−141.25	−160.60	−5.70	15.11
17	−98.28	−106.75	−4.08	5.96
18	−109.72	−117.33	−6.88	6.90
19	−127.61	−134.97	−6.68	5.96
20	−122.64	−136.70	−5.40	12.90
21	−117.89	−133.05	−4.88	13.50
22	−127.59	−143.45	−6.94	14.02
23	−139.80	−152.16	−0.92	9.91
24	−131.99	−147.49	−6.57	9.05
25	−121.09	−120.45	−5.89	−2.36
26	−146.98	−156.76	−6.65	6.92
27	−121.91	−130.30	−6.61	−0.05
28	−152.20	−157.85	−5.85	3.64
29	−151.30	−179.28	−3.10	16.21
Letrozole	−125.71	−130.48	−1.61	3.55

RESEARCH ARTICLE

3. RESULTS AND DISCUSSION

3.1. Molecular Docking Studies

Molecular docking of 1,2,3-triazole derivatives to the aromatase enzyme was performed to investigate their binding interactions and to explore their binding modes. Moreover, our lead compound was also docked in order to investigate its binding pattern to the aromatase active site. The Protein-Ligand interaction plays a vital role in structural based drug design.

In this present study, we have identified 1,2,3-triazole derivatives, by means of molecular docking studies to be a novel and likely more potent inhibitor of aromatase than one of third-generation aromatase inhibitors (letrozole).

The results obtained show that all the ligands have interactions with the 3EQM at the level of the cavity 1, the Figure 5 explain the interaction between human placental aromatase cytochrome P450 and most active compounds and Letrozole.

Table II. Summary of residues interacting with the aromatase inhibitors.

Interacting residues of receptor 3EQM			Interaction distance (Å)	Interaction strength (Kcal/Mol)
Letrozole	H-bond	arg192.....N	2.29	−1.17
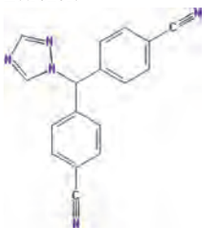		arg192.....N	3.14	−0.45
	Steric	Pro308.....C	3.16	0.84
		Arg192.....C	3.02	1.68
		Arg192.....C	2.65	3.92
		Arg192.....C	3.11	1.12
		Gln218.....C	3.07	1.41
		phe221.....C	3.09	1.30
		his480.....N	2.93	2.22
		val313.....C	3.11	1.16
		ASP309.....C	3.14	0.99
		ASP309.....C	3.20	0.63
		Ser478.....C	2.93	2.25
L14	H-bond	arg435.....N	2.86	−1.66
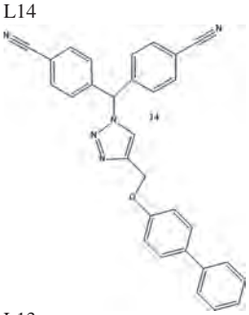		gly439.....N	3.05	−0.81
		trp141.....N	3.10	−2.35
	Steric	Leu152.....N	3.02	1.69
		Ala438.....N	3.03	1.62
		Thr310.....C	2.58	4.35
		Ala443.....C	2.77	3.20
L13	H-bond	arg145.....N	3.10	−2.49
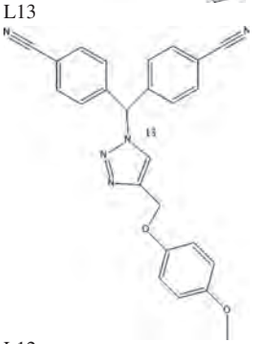		vol369.....O	2.86	−2.50
		val370.....O	2.73	−1.90
	Steric	Ser314.....C	3.07	1.41
		pro429.....C	3.09	1.27
		pro429.....C	3.03	1.65
		arg145.....C	3.19	0.68
L12	H-bond	ala438.....N	2.89	−0.68
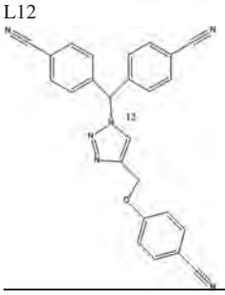		cys437.....N	3.45	−0.63
		cys437.....N	2.60	−2.25
		cys437.....N	2.41	−2.25
		gly439.....N	3.15	−2.25
		gly439.....N	2.60	−1.88
	Steric	Ile133.....C	3.16	0.83
		Trp141.....N	3.17	0.81
		Gly439.....N	3.16	0.83
		Met311.....C	3.09	1.29

RESEARCH ARTICLE

Based essentially on the comparison between the energies obtained using Mol Dock Score and the results obtained during molecular docking, it is noted that the energies of the complexes formed by ligands L14, L13, L12 are lower compared to other complexes. −179.89, −165.8 and 165.01 kcal/mol respectively. The energy map of 3EQM that might contribute in steric interaction favorable (green color), hydrogen acceptor favorable (turquoise color), hydrogen donor favorable (yellow color) and electrostatic potential of 3EQM (red and blue color) with the ligand viz. Letrozole, L14, L13, and L12 are shown in Figure 4, respectively.

The main type of interaction for the letrozole atom control is the steric interaction. On the other hand, the main interaction is hydrogen acceptor for the three studied compounds. Table II, illustrates this conclusion.

The docked structure of L14 indicated that the CN group was extensively hydrogen bonded to the arg435, and trp141 residues with bond distances of 2.86, and 3.10 Å respectively (Table I) (Fig. 6). Another nitrogen atom of compound L14, was also involved in a hydrogen bond interaction with the gly439 residue of the 3EQM. Additionally, leu152, ala438, thr310, and ala443 residues of the 3EQM displayed steric interactions with compound L14.

The compound 13 bearing methoxy substitution showed the second best ligand. The stereo view of the docked complex indicated that the compound L13 was extensively hydrogen bonded with the val370, val369 and arg145 residues of the 3EQM (Fig. 6).

Both CN and OCH_3 groups were involved in hydrogen bond formations with the residues of the 3qme. The CN group displayed hydrogen bonding with Arg145 (2.73 Å),

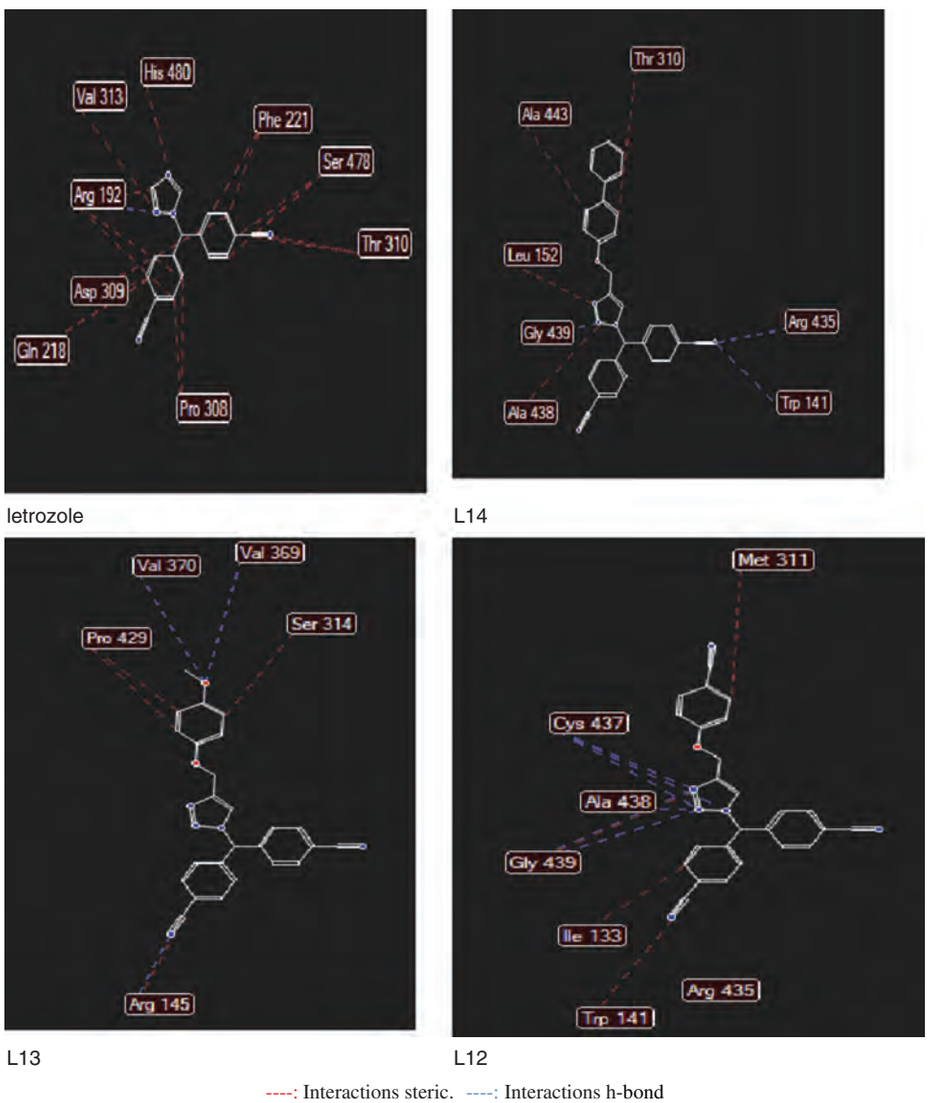

Fig. 6. Hydrogen bonding and steric interactions between aromatase receptor and most active compounds.

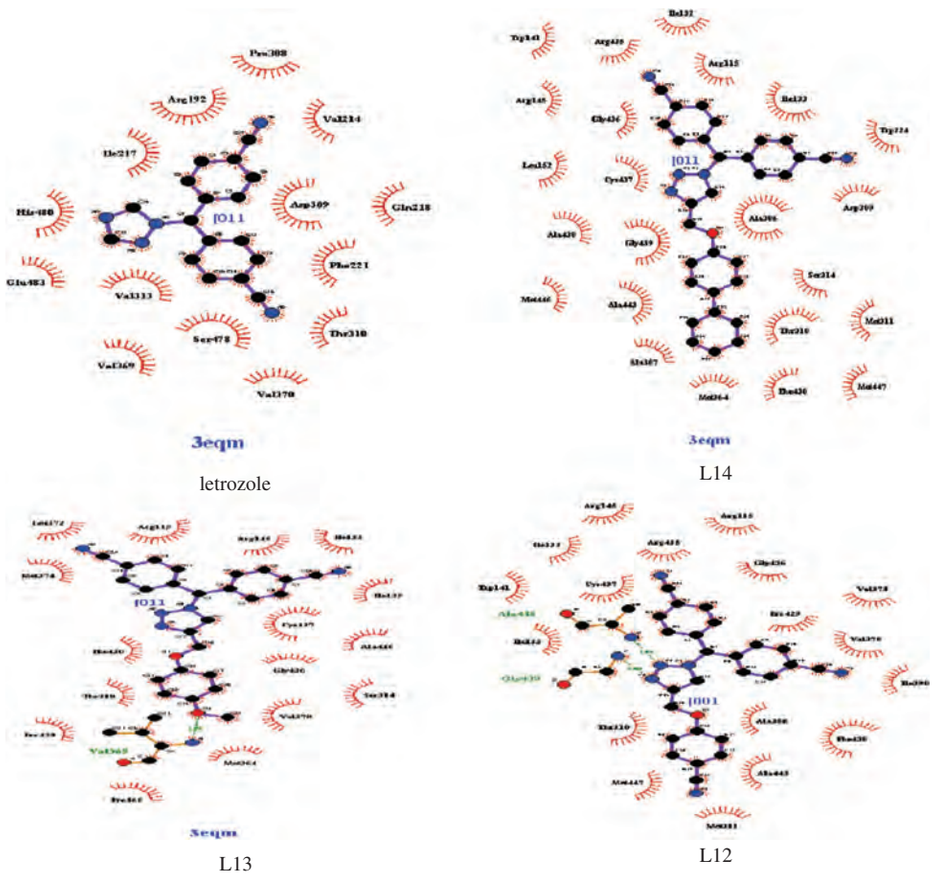

Fig. 7. Ligplot+ results showing the interactions of most active compounds and letrozole with 3EQM.

while the OCH_3 group was involved in hydrogen bond formations with Val370 (3.1 Å) and val369 (2.86 Å) residues. Other residues of 3EQM, viz. pro429 and ser314 demonstrated strong steric interactions with compound 13, (Fig. 7).

To confirm our results, we have shown in the Figure 6 the different interactions between the residues of the active site and the 4 ligands (fourth: letrozole ligand).

The distances measured between the 3 ligands and the amino acids of the cavity 1 are cited in the Table II.

The distances between the residues of the active site and the L14, L12, L13 vary between 2.58 Å and 3.45 Å, in this case it can be observed that according to Anne Imberty,[23] the interactions with distances between 2.5 Å and 3.1 Å Are considered strong, although those with distances between 3.1 Å and 3.55 Å are assumed to be average and when their distances are greater than 3.55 Å, they are considered to be weak.

Most of amino acid residues in hydrophobic active site were involved in affinity hydrophobic bonding interactions of ligand[24] (Figs. 8 and 9). This figure shows hydrophobic and electrostatic bonding between the most active compounds L14, L13, and L12 and letrozole with 3EQM.

The structure of most main content of 1,2,3-triazole was no polar, so this gave an advantage to hydrophobic for binding inside chains as receptor active site. The most

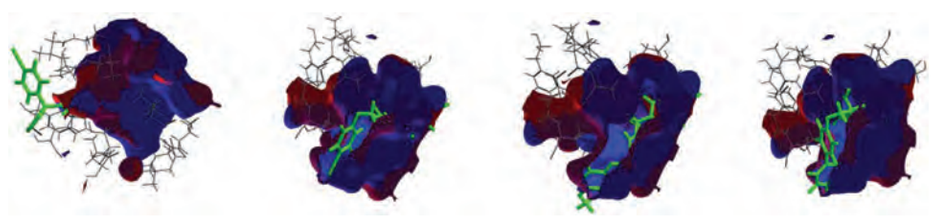

Fig. 8. Hydrophobic bonding interactions between human placental aromatase cytochrome P450 and most active compounds and letrozole.

RESEARCH ARTICLE

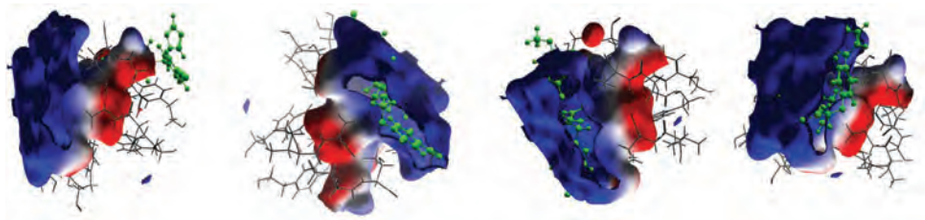

Fig. 9. Electrostatic bonding interactions between human placental aromatase cytochrome P450 and most active compounds and letrozole.

active compounds have similar role binding with letrozole that has been proven as aromatase agent and occupied in cavity 1 of human placental aromatase cytochrome P450 toward hydrophobic binding with aromatic ring, aliphatic chain and carbonyl group. Aromatic ring was important for binding.

3.2. Molinspiration Calculation

The *C*Log*P* (octanol/water partition co efficient) was calculated by the methodology developed by Molinspiration as a sum of fragment based contributions and correlation factors. The molecular descriptors of five compounds given in Table III were tested to Lipinski's rule of five, interestingly all the ligands which we selected have molecular weight in the range of 416–467 (<500). Low molecular weight drug molecules (<500) are easily transported. Diffuse and absorbed as compared to heavy molecules.[35]

Molecular weight is an important aspect in therapeutic drug action, if it increases correspondingly, it effects the drug action.[36] Number of hydrogen bond acceptors (O and N atoms) and number of hydrogen bond donors (NH and OH) in the tested compounds were found to be within Lipinski limit range from 5–7 and less than 10 and 5 respectively.

Lipophilicity (log*P* value) and TPSA values are two important properties for the prediction of oral bioavailability for drug molecules.[37] Permeability property of compounds were analyzed, the calculated log *P* value of L13 and L12 compounds was 4.49 and 4.18 (<5) respectively. In contrast, the oral bioavailability of L14 is questionable where the *m*log*p* was outranged. Which is the acceptable limit for the drugs to be able to penetrate through bio membranes.

Table III. *In-silico* prediction of ADME properties of compounds L14, L13 and L12.

Compound	Mi logP^C	TPSA^F	MW^D	HBA^A	HBD^B	N ROT^E
L14	6.22	87.54	467.54	6	0	7
L13	4.49	96.74	421.46	7	0	7
L12	4.18	111.13	416.44	7	0	6

Notes: ^{A}Number of hydrogen bond acceptors, ^{B}number of hydrogen bond donors, ^{C}calculated octanol/water partition coefficient, ^{D}molecular weight, ^{F}topological polar surface area, ^{E}number of rotatable bonds.

Topological polar surface area TPSA was calculated as described by Veber et al.[3] O- and N-centered polar fragment were considered. TPSA has shown to be a very good descriptor characterizing drug absorption. Including intestinal absorption, bioavailability, Caco-2 permeability and BBB penetration. The highest degree of lipophilicity was found with all the compounds, which are an indication for good lipid solubility that will help the drug to interact with the membranes. TPSA was calculated from the surface areas that are occupied by oxygen and nitrogen atoms and by hydrogen atoms attached to them.[38] Thus, the TPSA is closely related to the hydrogen bonding potential of a compound. In our study, all ligands exhibited 86–111 value of TPSA, indicates good bioavailability by oral route. Good bioavailability is more likely for compounds with $\leq$10 rotatable bonds and TPSA of $\leq$140 Å. As the number of rotatable bonds increases, the molecule becomes more flexible and more adaptable for efficient interaction with a particular binding pocket. Interestingly all the four compounds have 6–7 rotatable bonds and flexible.

3.3. ADMET Properties

As derived fromadmetSAR server, reveal that L14 and L13 had better Human Intestinal Absorption (HIA) score than the control letrozole. Greater HIA denotes that the compound could be better absorbed from the intestinal tract upon oral administration. The results obtained for BBB penetrability greatly agreed with structures of the studied compounds. The compound has a less polar sesquiterpene lactone, was predicted to cross BBB, this is their order (L12, L13, L14 and letrozole). When it comes to predicting the efflux by P-glycoprotein P-gp all the compounds came out as a non-substrate and non-inhibitor of P-gp similar to our control molecule. AMES toxicity test is employed to know whether a compound is mutagenic or not. Similar to the control molecule, all the test ligands displayed negative AMES toxicity test, which means that the ligands are non-mutagenic. Carcinogenic profile also revealed that the ligands were non-carcinogenic similar to the control molecule.

The next important parameter is cytochrome P450 (CYP), which is known as isozymes group and it is involved in the metabolism of drugs, fatty acids, steroids,

RESEARCH ARTICLE

Table IV. ADMET predictions using AdmetSAR.

	L14		L13		L12		Letrozole	
Mode	Result	Probability	Result	Probability	Result	Probability	Result	Probability
				Absorption				
Blood-brain barrier	BBB+	0.9732	BBB+	0.9564	BBB+	0.9746	BBB+	0.9737
Human intestinal absorption	HIA+	1.0000	HIA+	1.0000	HIA+	0.9971	HIA+	0.9965
Caco-2 permeability	Caco2+	0.5053	Caco2+	0.5369	Caco2+	0.5178	Caco2+	0.6347
P-glycoprotein substrate	Non-substrate	0.7781	Non-substrate	0.7222	Non-substrate	0.7669	Non-substrate	0.8391
P-glycoprotein inhibitor	Non-inhibitor	0.7162	Non-inhibitor	0.7230	Non-inhibitor	0.7059	Non-inhibitor	0.8087
	Inhibitor	0.5778	Non-inhibitor	0.6170	Non-inhibitor	0.5736	Non-inhibitor	0.9147
Renal organic cation transporter	Inhibitor	0.5603	Inhibitor	0.5994	Inhibitor	0.6093	Non-inhibitor	0.5908
Renal organic cation transporter	Inhibitor	0.5603	Inhibitor	0.5994	Inhibitor	0.6093	Non-inhibitor	0.5908
				Distribution				
Subcellular localization	Mitochondria	0.8808	Mitochondria	0.8460	Mitochondria	0.8475	Mitochondria	0.7175
				Metabolism				
CYP450 2C9 substrate	Non-substrate	0.7090	Non-substrate	0.6527	Non-substrate	0.7134	Non-substrate	0.7898
CYP450 2D6 Substrate	Non-substrate	0.8224	Non-substrate	0.8163	Non-substrate	0.8220	Non-substrate	0.9116
CYP450 3A4 substrate	Non-substrate	0.5248	Substrate	0.5232	Non-substrate	0.5470	Non-substrate	0.6843
CYP450 1A2 inhibitor	Inhibitor	0.6730	Inhibitor	0.5711	Inhibitor	0.6088	Non-inhibitor	0.8374
CYP450 2C9 Inhibitor	Inhibitor	0.6980	Non-inhibitor	0.5246	Inhibitor	0.5946	Non-inhibitor	0.9071
CYP450 2D6 Inhibitor	Non-inhibitor	0.8416	Non-inhibitor	0.8758	Non-inhibitor	0.8549	Non-inhibitor	0.9230
CYP450 2C19 inhibitor	Inhibitor	0.7239	Non-inhibitor	0.5319	Inhibitor	0.6457	Inhibitor	0.8993
CYP450 3A4 inhibitor	Inhibitor	0.5000	Non-inhibitor	0.5256	Non-inhibitor	0.5834	Inhibitor	0.6451
CYP inhibitory promiscuity	High CYP inhibitory promiscuity	0.8693	High CYP inhibitory promiscuity	0.6872	High CYP inhibitory promiscuity	0.7543	High CYP inhibitory promiscuity	0.7027
				Excretion				
				Toxicity				
Human ether-a-go-go-related gene inhibition	Weak inhibitor	0.6477	Weak inhibitor	0.5000	Weak inhibitor	0.5267	Weak inhibitor	0.9261
	Non-inhibitor	0.7219	Non-inhibitor	0.7748	Non-inhibitor	0.7539	Non-inhibitor	0.8817
AMES toxicity	Non AMES toxic	0.5678	AMES toxic	0.5240	Non AMES toxic	0.5270	Non AMES toxic	0.6371
Carcinogens	Non-carcinogens	0.8990	Non-carcinogens	0.9274	Non-carcinogens	0.9169	Non-carcinogens	0.8926
Fish toxicity	High FHMT	0.9872	High FHMT	0.8696	High FHMT	0.9623	High FHMT	0.9605
Tetrahymena pyriformis toxicity	High TPT	0.9389	High TPT	0.9257	High TPT	0.9136	High TPT	0.8526
Honey bee toxicity	Low HBT	0.6900	Low HBT	0.6802	Low HBT	0.6630	Low HBT	0.7787
Biodegradation	Not ready biodegradable	0.9897	Not ready biodegradable	0.9585	Not ready biodegradable	0.9787	Not ready biodegradable	0.9864

bile acids and carcinogens. Notwithstanding, some of the cytochrome P450 isoforms could be inhibited by one or more of the tested compounds.

Considering the cytochrome P450 (CYP) analysis, the major limitation of letrozole is its CYP450 3A4 substrate nature, lead to high drug–drug interaction and interruption in the metabolism of the drug combination. The compound L13 overcomes that limitation. Generally, the predicated ADMET properties for derivatives suggest that these derivatives can be possible inhibitors of 3EQM enzymes with desirable pharmacokinetic properties.

4. CONCLUSION

All the compounds were found to have a high degree of lipophilicity, which indicates a good lipid solubility that will help the drug to interact with the membranes. The analysis of molecular docking gives place at the prospective identification of ligands. The molecules L14, L13 and L12 have the potential to inhibit the activity of 3EQM. The molecules L14, L13 and L12 demonstrate the better result in *in-silico* analysis. Moreover L14 has shown good hydrogen bonding which was not observed in our prototype Letrozole. All the designed ligands have shown no trace of carcinogenic. Moreover L14, L13 and L12 have shown mutagenic property. Hence it has been predicted that all our designed ligands can possibly act as new leads for the treatment of estrogen dependent diseases like endometriosis and breast cancer.

References and Notes

1. E. K. Tiburu, M. Mutocheluh, P. K. Arthur, P. W. Narkwa, A. A. Salifu, M. A. Agyei, R. Yeboah, H. N. A. Fleischer, J. Zhuang, and G. Awandare, *J. Biomater. Tissue Eng.* 7, 544 (**2017**).
2. A. Jemal, F. Bray, M. M. Center, J. Ferlay, E. Ward, and D. Forman, *CA Cancer J. Clin*. 61, 69 (**2011**).
3. W. R. Miller, *Semin. Oncol*. 30, 3 (**2003**).
4. G. L. Smith, Y. Xu, T. A. Buchholz, S. H. Giordano, J. Jiang, Y. C. Shih, and B. D. Smith, *JAMA* 307, 1827 (**2012**).
5. J. A. Cox and T. A. Swanson, *Nat. Rev. Clin. Oncol*. 10, 344 (**2013**).
6. F. Caporuscio, G. Rastelli, C. Imbriano, and A. Delrio, *J. Med. Chem*. 54, 4006 (**2011**).
7. J. Geisler, N. King, M. Dowsett, L. Ottestad, S. Lundgren, and P. Walton, *Br. J. Cancer* 74, 1286 (**1996**).
8. C. J. Fabian, *J. Clin. Oncol*. 23, 1644 (**2005**).
9. Z. L. Wei, J. Yang, F. M. Li, W. Q. Peng, D. Xie, L. B. Qiu, and J. M. Zhao, *J. Biomater. Tissue Eng.* 7, 696 (**2017**).
10. G. Yang, Z. Li, H. Zhao, M. Zhang, and D. Sun, *J. Biomater. Tissue Eng.* 7, 708 (**2017**).
11. M. Dowsett, *Clin. Endocrinol*. 32, 623 (**1990**).
12. M. Dowsett, *J. Steroid. Biochem. Mol. Biol*. 95, 167 (**2005**).
13. P. E. Goss and K. Strasser, *J. Clin. Oncol*. 19, 881 (**2001**).
14. A. D. Favia, O. Nicolotti, A. Stefanachi, F. Leonetti, and A. Carotti, *Expert Opin. Drug Discov.* 8, 395 (**2013**).
15. M. A. C. Neves, T. C. P. Dinis, and G. Colombo, *J. Med. Chem*. 52, 143 (**2009**).
16. J. Doiron, A. H. Soultan, R. Richard, M. M. Toure, N. Picot, R. Richard, C. M. Uperlovic, G. A. Robichaud, and M. Touaibia, *Eur. J. Med. Chem*. 46, 4010 (**2011**).
17. H. Zhang, L. Zhao, C. Deng, N. Dong, and J. Shi, *J. Biomater. Tissue Eng*. 7, 735 (**2017**).
18. S. Medjahed, S. Belaidi, S. Djekhaba, N. Tchouar, and A. Kerassa, *J. Bionanosci*. 10, 118 (**2016**).
19. S. Khamouli, S. Belaidi, Z. Almi, S. Medjahed, and H. Belaidi, *J. Bionanosci*. 11, 301 (**2017**).
20. F. Soualmia, S. Belaidi, H. Belaidi, N. Tchouar, and Z. Almi, *J. Bionanosci*. 11, 584 (**2017**).
21. S. Nithiyanantham, L. Palaniappan, and M. Lenin, *J. Bionanosci.* 9, 359 (**2015**)
22. Xi. Liu, R. Zhu, Y. Zhang, Y. Xue, and H. Fan, *J. Biomater. Tissue Eng*. 7, 1 (**2017**).
23. J. Campos, C. Jimenez, C. Trigo, P. Ibarra, D. Rana, R. Thiruganesh, M. Ramalingam, and Z. S. Haida, *J. Bionanosci*. 9, 249 (**2015**).
24. K. Dermeche, N. Tchouar, S. Belaidi, and T. Salah, *J. Bionanosci*. 9, 395 (**2015**).
25. D. Ghosh, J. Griswold, M. Erman, and W. Pangborn, *Nature* 457, 219 (**2009**).
26. C. Nantasenamat, A. Worachartcheewan, S. Prachayasittikul, C. Isarankura-Na-Ayudhya, and V. Prachayasittikul, *Eur. J. Med. Chem.* 69, 99 (**2013**).
27. V. R. Avupati, P. N. Kurre, S. R. Bagadi, M. K. Muthyala, and R. P. Yejella, *Biopharmaceutical Descriptors* 10, 74 (**2010**).
28. R. Storn and K. Price, Tech.-Report, International Computer Science Institute, Berkley (**1995**).
29. C. A. Lipinski, F. Lombardo, B. W. Dominy, and P. J. Feeney, *Adv, Drug Deliv. Rev*. 46, 3 (**2001**).
30. D. F. Veber, S. R. Johnson, H. Y. Cheng, B. R. Smith, K. W. Ward, and K. D. Kopple, *J. Med. Chem*. 45, 2615 (**2002**).
31. F. Cheng, W. Li, Y. Zhou, J. Z. S. Wu, G. Liu, P. Lee, and Y. Tang, *Chem. Inf. Model*. 52, 3099 (**2012**).
32. M. A. Neves, T. C. Dinis, G. Colombo, and M. L. S. Melo, *J. Med. Chem*. 52, 143 (**2009**).
33. A. Imberty, C. Gautier, J. Lescar, S. Perez, L. Wyns, and R. Loris, *J. Biol. Chem*. 275, 17541 (**2000**).
34. R. Chakrabarti, A. M. Klibanovt, and R. A. Friesner, *National Academy of Sciences* 102, 10153 (**2005**).
35. B. R. P. Kumar, S. Mukesh, U. B. Bhikhalal, R. I. Kakkot, J. Meghana, B. Praveen, and M. J. Nanjan, *Med. Chem. Res*. 19, 984 (**2010**).
36. V. Srimai, M. Ramesh, K. Satya, and P. T. Parthasarathy, *Med. Chem. Res*. 22, 5314 (**2013**).
37. J. Kelder, P. D. Grootenhuis, D. M. L. P. Delbressine, and J. P. Ploemen, *Pharm. Res*. 16, 1514 (**1999**).
38. P. Ertl, B. Rohde, and P. Selzer, *J. Med. Chem*. 43, 3714 (**2000**).

Received: xx Xxxx xxxx. Accepted: xx Xxxx xxxx.